

# Through-Wafer Interconnects for High Degree of Freedom MEMS Deformable Mirrors

Alioune Diouf<sup>1</sup>, Thomas G. Bifano<sup>1</sup>, Jason B. Stewart<sup>2</sup>, Steven Cornelissen<sup>2</sup>, Paul Bierden<sup>2</sup>

<sup>1</sup>Boston University Photonics Center, 8 Saint Mary's Street, Brookline, MA 02446, USA

<sup>2</sup>Boston Micromachines Corporation, 30 Spinelli Place, Cambridge, MA 02138

## Abstract

The development of an assembly and packaging process for MEMS deformable mirrors (DMs) with through wafer via (TWV) interconnects is presented. The approach consists of attaching a DM die with high-density TWV electrostatic actuator interconnects to an interposer substrate that fans out these connections for interfacing to conventional packaging technology.

## 1. Introduction

Boston University MEMS DMs are surface-micromachined polysilicon double-cantilever actuator architecture commercialized by Boston Micromachines (BMC). This architecture (Figure 1) is based on an array of electrostatically powered actuators that support the compliant mirror facesheet through a small attachment post at the center of each actuator. This architecture is used on a family of DM including the 1024 actuators (32x32) on a square pitch of about 300  $\mu\text{m}$ , and the 4096 element DM under development by Boston Micromachines [1] to allow for high-order wavefront aberrations correction to achieve contrast ratios of  $10^7$ – $10^8$ . As the demand for actuator grows, innovative packaging method will be required in order to preserve one of the key advantages provided by the use of MEMS DMs: size.

The approach used for packaging commercial MEMS DM arrays to date has been to dedicate one or more MEMS layers to wire routing, and to use these routing lines to connect electrostatic actuator electrodes to a ring of lithographically-defined, gold-coated bond pads at the periphery of the MEMS die. After bonding the MEMS die into a cavity in a custom-manufactured ceramic chip carrier, each bond pad is connected to corresponding pad on the ceramic package using an automated wire bonding tool. This approach means that the die area required for the device grows in proportion to the square of the number of actuator, therefore reaches its scalability limit at actuator counts of  $\sim 4000$  around the perimeter of a 2" wide die. Moreover, MEMS layer dedicated to wire routing lines is particularly susceptible to yield problems. Since wire routing lines are sized and spaced at the resolution limits of the fabrication process, processing defects and contamination tend to cause yield failures in this layer. Flip-chip assembly of TWV DMs and interposer die therefore represents a fundamental process step needed for the realization of DMs with up to 10,000 actuators.

Through wafer via (TWV) allows the integration of sensors or actuators with their associated addressing and control circuitry. At least one foundry aims at making the process an industry standard [2, 3], and its application for optical MEMS devices has been previously studied by researchers at Sandia National Laboratories [4]. Gold thermo-compression bonding has been a standard in IC packaging [5, 6] and, along with the TWV method, is evaluated in this work for high actuator count MEMS DM packaging.

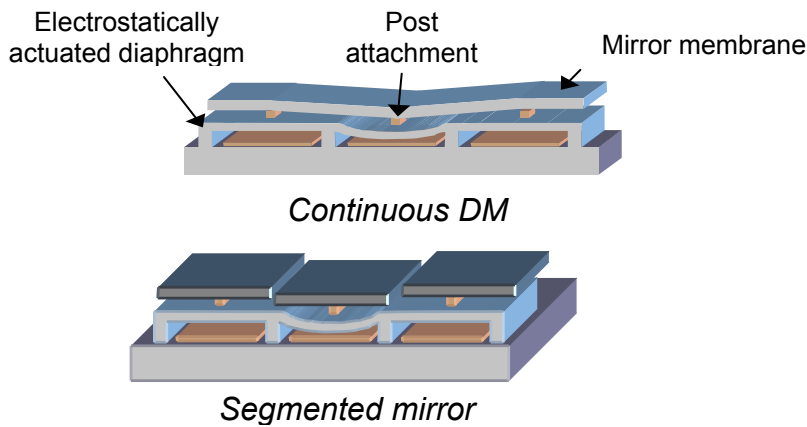


**Figure 1:** BU MEMS DM architecture: the continuous facesheet (top) and segmented mirror (bottom).

## 2. Flip-chip bonding system

The FC-150 flip-chip bonding process starts with mounting the “chip” and “substrate” to be bonded. The parts are mounted on the Universal Bonding Arm (UBA) and chuck, respectively, as illustrated in Figure 2. For the process described herein, the interposer die is located at the “chip” position, and the TWV die is located at the “substrate” location. If the entire back side of the die at the chip position can tolerate the applied system vacuum, which is the case for backside of the interposer die, then the FC-150 vacuum pick can also be used, which is an automated method for selecting die to be bonded from their carrier.

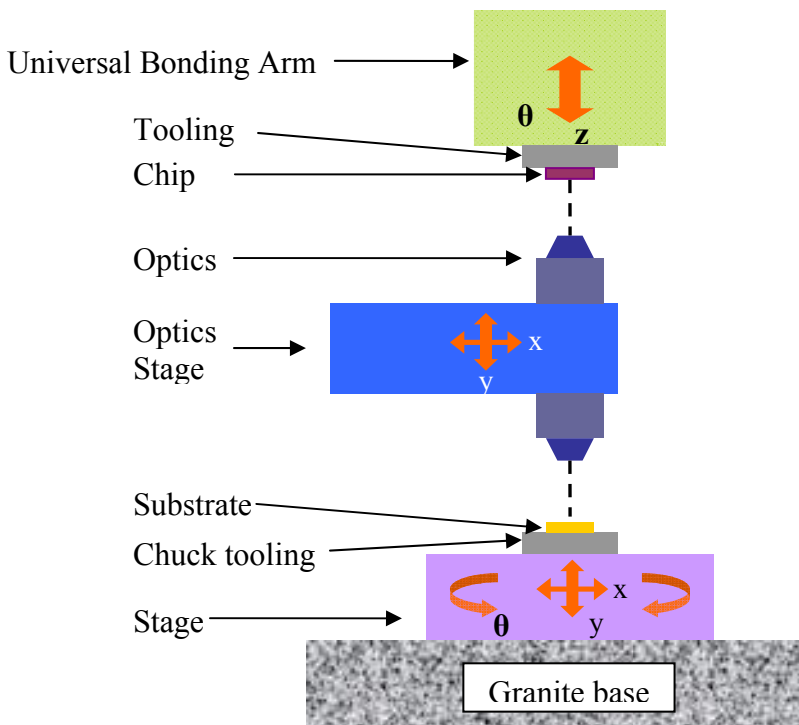


**Figure 2:** Illustration of FC-150 system and chip/substrate alignment degrees of freedom.

The FC-150 chuck and UBA vacuum tooling is custom made to fit the die to be bonded. The tooling material selected is specific to the type of flip-chip bonding process performed. Silicon carbide tools are suitable for high heat and high force bonding application, such as gold-gold thermo-compression bonding. Invar 36 is another material suitable for this purpose and can be quickly manufactured within the BU research facility. As part of this work, two high-precision silicon carbide and Invar 36 tools were fabricated to vacuum hold both the TWV die (substrate) and interposer die (chip) - shown in Figure 3. Design considerations for the DM tool includes the presence of peripheral bond pads and their geometry, the size of the mirror surface, and the geometry of the die itself, a cross-section of which can be seen in Figure 4. The bond pads and associated wire traces were present in these first generation devices for testing purposes, although will not be included in future fabrication runs. As seen in Figure 4, they reduce the surface area of the chip where bonding pressure is applied, they complicate placement of the die in the tooling fixture, and the wire traces influence alignment planarity.

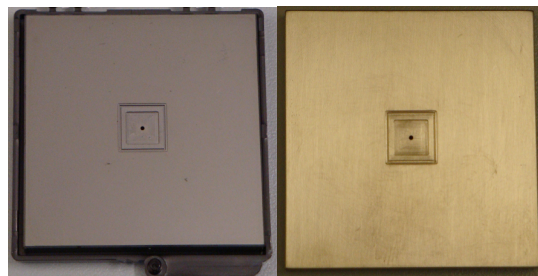


**Figure 3:** Final silicon carbide tool (left). Low thermal expansion Invar 36 tool fabricated in-house (right).

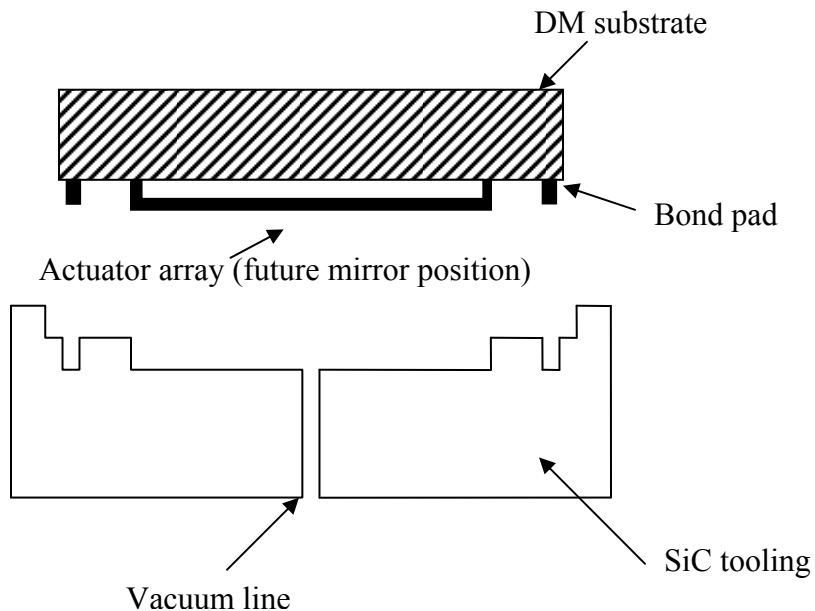


**Figure 4:** Cross section of silicon carbide tool (bottom) designed for DM electrostatic actuator array with TWV interconnects (top – upside down).

Once the parts are mounted in their respective vacuum tooling, an accurate alignment procedure is required prior to bonding. During the bonding process, the samples are first preheated at a temperature that allows for expansion of the substrate and chip, and are then aligned. The FC-150 can position the parts in six degrees of freedom. The chuck positions the TWV die in the x- and y-axis and can also rotate it about the z-axis ( $\theta$ ). The step resolutions in the lateral and rotational degrees of freedom are 100nm and 9 $\mu$ rad, respectively.

In the x- and y- direction, the system uses a bi-directional optical microscope (Figure 2 - center) to locate the user's alignment marks on the chip and substrate. For parallelism, two options are available. The first is an autocollimator that projects an image of a cross onto the chip and substrate. By overlaying the cross reflected from the upper part to the one from the lower part (reference), the leveling can be adjusted. The second option involves an advanced laser leveling method that uses a laser to measure the distance between the two parts (chip and substrate) at three different locations. The user then adjusts the leveling until the three distances matches. This option is used for auto-collimation in the absence of a reflective surface, when the cross reflection is not very sharp.

Following substrate and chip mounting and alignment, the final bonding step consists of mating the two parts. During this phase of bonding complete control of the heating rate is possible, and both substrate and chip temperature can be controlled independently. All bonding methods require an applied force, while the addition of heat or UV energy is optional, and depends on the type of bonding, such as fusion, anodic, thermo-compression or adhesives. To perform thermo-compression bonding using gold studs or bumps as the bonding material, force and heat are required to form a successful bond. The chuck and UBA use a halogen lamp located below the tooling to control temperature from room temperature to 450C. After bonding takes place, the tool and bonded assembly can be cooled either passively or with nitrogen jet.

The bonding force is applied by driving the UBA (with chip and tooling) down to the substrate. A maximum mass of 50kg can be applied with the UBA with control over the time of application, the rate of increase, and the periods during which the force increases decreases or remains constant. After the bonding time elapses, the cooling process (passive or active jet blowing) commences immediately followed by the release of the chip from the chuck tooling. This release is executed by shutting down the vacuum and retracting the bonding arm to its original position leaving the chip on top of the substrate.

### **3. Gold stud bumping process**

Gold-gold thermo-compression bonding was the primary flip-chip assembly process explored in this work. Gold was selected for the bonding interface primarily due to its low yield stress, corrosion resistance and high electrical conductivity. The bond pad arrays on the backside of the actuator device die (the TWV interconnects) and on the surface of the interposer die consist of 200 $\mu$ m diameter circles on a 400 $\mu$ m square pitch. The thickness of each bond pad is approximately 50nm. To accommodate for planarity errors between the surfaces of the two die and to improve the adhesion of adjoined bond pads, an array of gold studs or bumps are placed on the interposer die prior to bonding. This is performed using an Esec 3018 automated wire bonding system. The use of gold studs in adhesive bonding also helps to provide strength to the bond sties, as well as physical spacers between bonded die that can help prevent shorting.

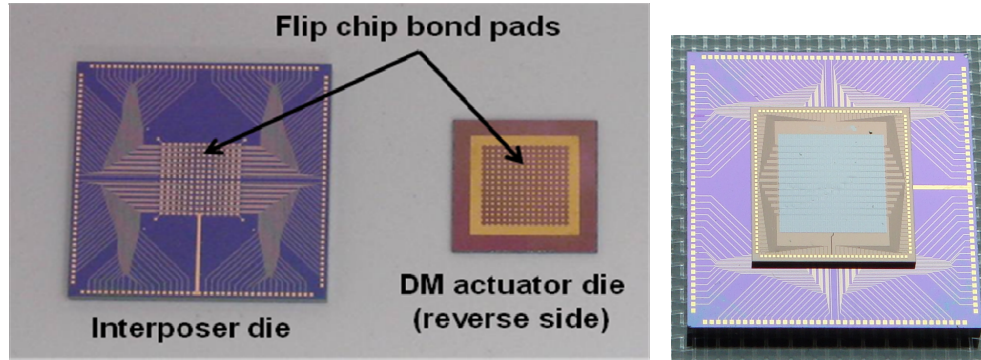


**Figure 5:** Gold bond pad arrays on the interposer die and reverse side of the TWV die (left) to be aligned and bonded using the thermo-compression process (right). Gold bumps are deposited on the interposer bond pads prior to being bonded.

The Esec wire bonder can be equipped with special bump bonding wire and capillaries to produce arrays of nearly identical cylindrical gold studs, which is ideal for bonding very high density interconnects. It is also capable of placing these bumps with sub-micron lateral precision. For the bumping process developed in this work, standard ball-wedge wire bonding capillaries were used and were capable of producing bumps consistently with similar size, but with very large tails, as shown in Figure 6. These tails are not ideal for high density studs, and can be significantly reduced by changing the type of capillary used. Regardless, the geometry of the gold bump was not critical for the flip-chip bonding process presented here as long as the bump was constrained within the allocated bond pad, which was consistently the case. Furthermore, any deviations or irregular shaping of the studs are compensated by the compliance of the heated material. It is therefore not necessary for the surfaces of the chip and substrate to be perfectly parallel as each bump gets flattened as much as needed to compensate for the initial non-planarity. The bumping process developed in this work used a 25  $\mu\text{m}$  diameter gold wire, and produced bump sizes ranging from 70 to 80  $\mu\text{m}$  in diameter and 50 to 80  $\mu\text{m}$  in height.

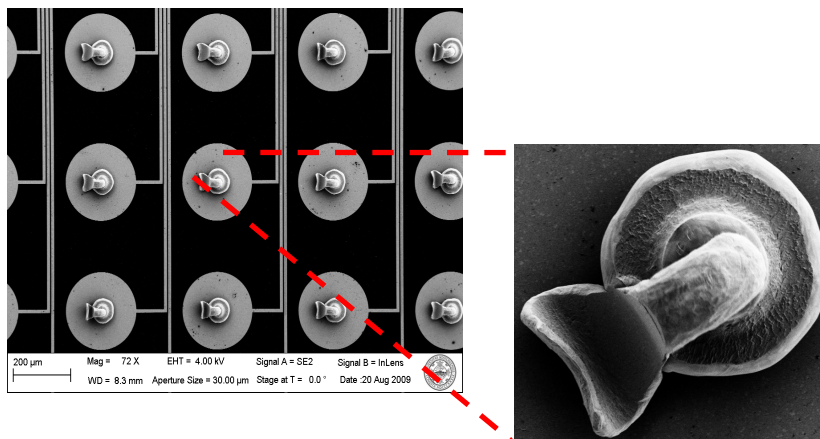


**Figure 6:** SEM images of (left) gold bump array (4x3 shown) on interposer gold pads and (right) a single gold bump tilted 25 degrees to show details.

#### 4. Thermo-compression bonding process development

Prior to flip-chip bonding fully functional TWV and interposer die, several thermo-compression experiments were first performed on silicon die patterned with 14x14 bond pad arrays. Die production involved coating double polished silicon wafers with thin films of chrome (50nm) for adhesion, and gold (150nm) for the bond pad layer. The thin film stack was patterned into bond pad arrays with identical geometry to the TWV and interposer die bond pads (200um diameter, 400um pitch) using standard photolithography. The die mask layout can be seen in Figure 7. After patterning, the wafers were diced into 10mm square die and covered with arrays of gold bumps (one bump per bond pad). The bumps were deposited using the optimized bumping recipe presented above. After bumping, a variety of thermo-compression bonding experiments were performed using the FC-150, where silicon test die without bumps were flip-chip bonded to die with bumps. The standard instrument vacuum tooling was used for these experiments, which applies a uniform bonding load to the reverse side of the chip stack after mating.

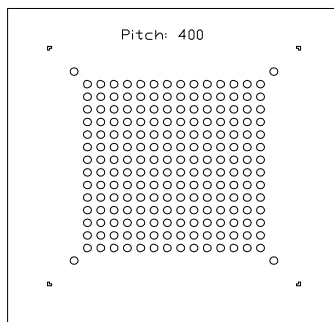


**Figure 7:** Bond pad layout for preliminary thermo-compression flip chip bonding experiments.

The goal for these preliminary bonding experiments was to find a suitable range of bonding temperatures and pressures capable of bonding two die successfully. Stress evaluation was only performed qualitatively. In other words, these experiments were aimed at obtaining baseline values for the necessary temperature, pressure, and bonding time required to produce a successful bond. Various silicon to silicon samples were successfully bonded at temperatures ranging from 250°C to 350°C, forces ranging from 400g to 15kg, and a bonding time ranging from 10 seconds to 30 seconds. Of these three parameters, it appears that temperature is the most critical for achieving adhesion. For example, samples heated below 200°C could not be bonded. Furthermore, it was determined that the removal of organics, typically through a UV-ozone clean, improves bonding adhesion at temperatures lower than 300°C.

The samples bonded in these experiments were used to evaluate the mechanical deformation of gold bumps and parallelism of bonded samples. A scanning electron microscope image (SEM) of a bond between two silicon chips can be seen in Figure 8. The bump started with a 70um height prior to bonding and resulted in a 20um gap after bonding, demonstrating sufficient bump deformation to yield an electrical connection between bond pads. The SEM cross sections of all inspected samples also show that parallelism between the die was maintained to less than 10nm. Bump profiles were also evaluated after destructively separating a previously bonded sample. The results shown in Figure 8 suggest the variation in the height of post bonded bumps is on the order of 100nm.

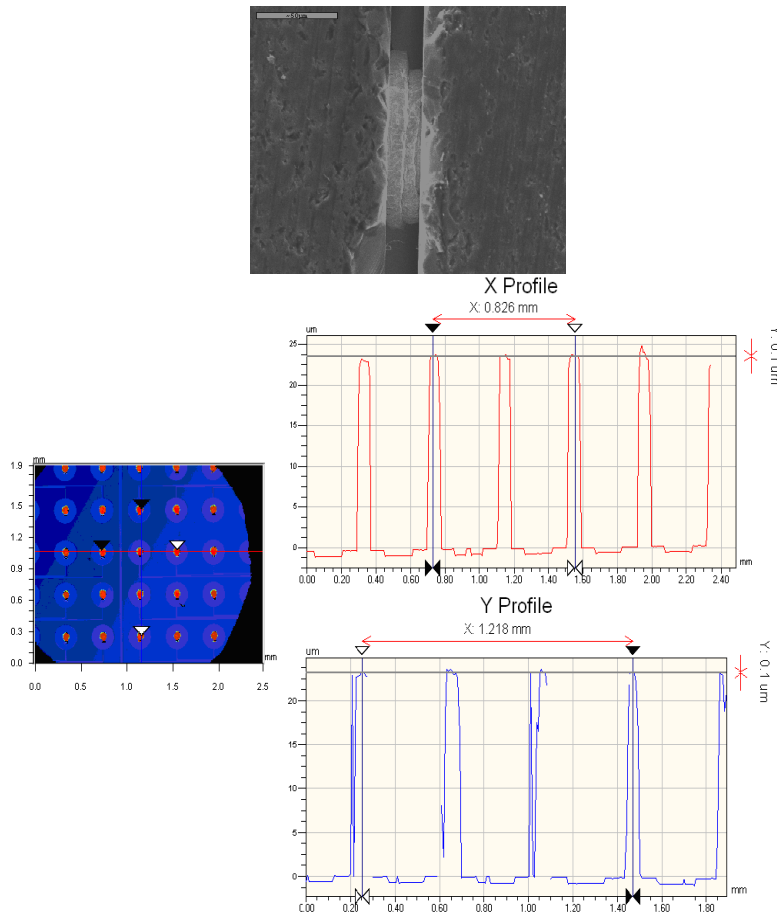


**Figure 8:** Cross section of a single gold bump between two silicon test die (top) and profile of post-bonded gold bumps used to evaluate chip-substrate parallelism (bottom).

### *TWV to interposer die bonding*

From the preliminary bonding experiment results, a baseline process was identified for the TWV and interposer die. It consisted of initial heating to 150°C for alignment, followed by additional heating to the bonding temperature (250°C -300°C) over a 10-30 second period, substrate-chip contact using a bonding force between 2 to 10kg for 10-30 seconds, and then cooling. Using these baseline parameters, illustrated in Figure 9, several test bonds were first performed on TWV and interposer die to evaluate the effectiveness of the test sample process on these different devices using the new custom tooling. These results were then used to develop a design of experiment (DOE) for identifying an ideal bonding recipe.

Several variables were used to characterize the quality of the flip-chip bonding process, including the electromechanical yield of the bonded actuator array, as well as residual stress in the bonded TWV die. Management of this stress is very important for maintaining the surface figure of future flip-chip bonded DMs. Due to the fact that the TWV die used in this work only contained actuator arrays, stress in the bonded die was evaluated through changes in substrate curvature, as well as unpowered actuator displacement. Change in die curvature provides a quantitative measure of the change in average residual stress in the die, where a change in actuator sag provides information about the local distribution of this stress.

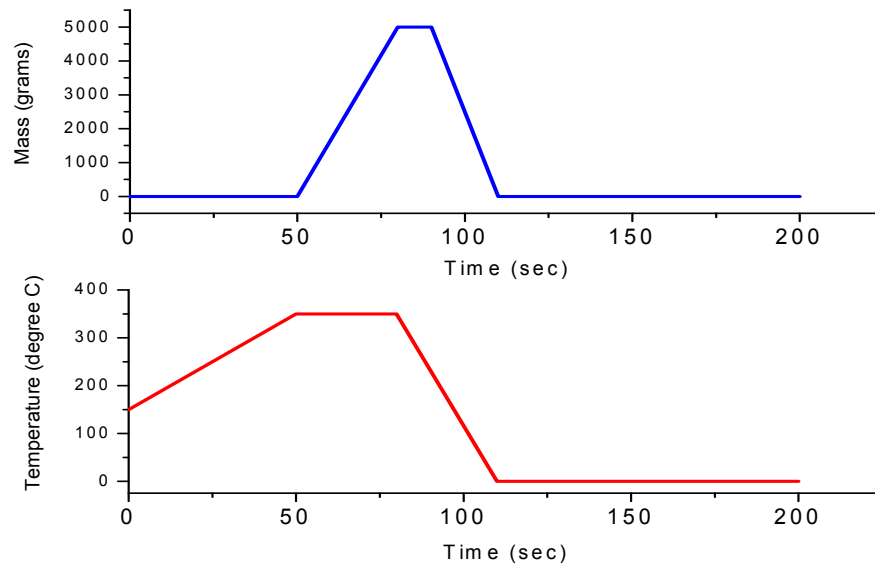


**Figure 9:** Sample temperature and bonding force profiles for thermo-compression bonding of TWV and interposer die.

The first TWV and interposer die bonding experiments suggested that survivability of the actuators was mostly influenced by the applied pressure. It was determined that an applied mass greater than 10kg destroyed most, if not all, of the actuators. It was also determined during these experiments that a cooling mechanism used after bonding led to actuator damage. The FC-150 uses a nitrogen cooling jet that blows gas on the reverse sides of the chip and substrate after bonding, which is undesirable in this application because the reverse side of the TWV die contains the fragile electrostatic actuator array. This jet of cooling nitrogen resulted in actuator damage and was disabled prior to further sample bonding. The only downside to this is waiting several minutes (3-5) instead of less than 1 minute for the cooling cycle to complete. Figure 10 shows an image of a successfully bonded TWV and interposer die, packaged and wire bonded in a 160 PGA carrier for electromechanical testing.

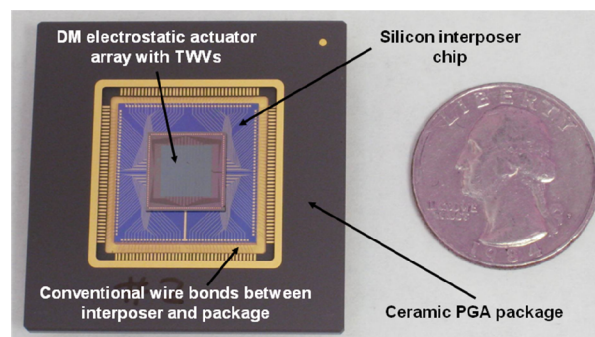


**Figure 10:** A bonded TWV and interposer die, packaged and wire bonded in a 160pin PGA chip carrier for electromechanical testing of the device actuator array.

Following the initial evaluation of flip-chip bonding parameters for the TWV and interposer die, an 8 run, 3 factor, 2 level, full factorial design of experiments (DOE) was performed using the FC-150. The three factors used were bonding time, bonding temperature and bonding force. The metric used to evaluate



bond quality was the change in TWV die radius of curvature, which is a quantitative measure of residual stress in the bonded die. The purpose of the DOE was to identify the influence of these parameters on bond quality from inferred values for die stress. Curvature change was measured using a surface mapping interferometric microscope, the Zygo NewView 6000, which can measure surface topography with sub-nm precision. The maximum radius of curvature profile measured across the 12x12 actuator area was used in the DOE. The DOE response factor is the change in curvature before and after bonding.

The input factors and levels for the DOE, selected using the preliminary bonding experiments, are summarized in Table 1:

**Table 1:** Process window for DOE experiments.

<i>Bonding parameter</i>	<i>Low (-1)</i>	<i>High (+1)</i>
Peak Force (grams)	2000	10000
Temperature (C)	250	350
Time at Peak (s)	10	30

The constants for the DOE were the initial temperature and the 55 second ramp to the max temperature. Results of the curvature change measurements and DOE run orders are shown in Table 2:

**Table 2:** Curvature measurements for first-order model.

<i>Sample #</i>	<i>Run Order</i>	<i>Bonding Temp (x<sub>1</sub>)</i>	<i>Force (x<sub>2</sub>)</i>	<i>Bonding Time (x<sub>3</sub>)</i>	<i>Curvature change (y) (m)</i>
3	1	-1	1	-1	7
1	2	-1	-1	-1	3.5
4	3	1	1	-1	6.8
6	4	1	-1	1	5
7	5	-1	1	1	6.5
8	6	1	1	1	7
5	7	-1	-1	1	2
2	8	1	-1	-1	3.5

The experimental run combinations following randomization are shown in Table 3. Standard errors are based on total error with 4 degrees of freedom (DF). The analysis of variance (ANOVA) table partitions the variability in curvature change into separate pieces for each of the main effects. The DOE has three main effects therefore 3 degrees of freedom. Each effect has two levels (+1, and -1) for a total 8 response combinations ( $2^3$ ), therefore 7 degrees of freedoms ( $2^3-1$ ). The column labeled “Coefs” are the coefficient for the linear regression, “SE Coef” is the square errors of the coefficients, “F” is the ratio of explained to unexplained variance, and “T, P” are standard stats for hypothesis testing. The DOE tests the statistical significance of each effect by comparing the mean square against an estimate of the experimental error. The *R*-squared statistic indicates that the first-order model explains 87.7% of the variability in curvature change. The equation of the fitted model in coded or dimensionless units is:

$$y = 0.4215 x_1 + 1.6625 x_2 - 0.0375 x_3 + 5.1265 \quad (1)$$

Since the *P*-value in the ANOVA table (Table 3,  $P = 0.027$ ) is less than 0.05, there is a statistically significant relationship between the variables or main effects at the 95% confidence level. We confirm that the bonding force influences curvature the most. In fact the *P*-values for the bonding temperature

(0.268) and bonding time (0.913) are not statistically significant at the 95% or higher confidence level. In other words, to a first-order, the bonding force alone can predict the curvature change of die. Regardless, the other two parameters are still included for prediction of an ideal bonding process, even if their effect on the curvature change cannot be determined at this confidence level. In sum, the results of the DOE suggest that the optimum gold thermo-compression bonding recipe for the TWV and interposer die are 5500g applied bonding mass for 10 seconds at an equilibrium temperature of 325C.

**Table 3:** Analysis of variance and factorial fit for DOE.

Analysis of variance				
Source	DF	Seq SS	F	P
Main Effects	3	23.484	9.5	0.027
Residual Error	4	3.295		
Total	7	26.77		

**Estimated effects and coefficient for curvature change (coded units)**

Term	Effect	Coefs	SE Coef	T	P
Constant		5.1625	0.3209	16.09	0
Bonding Temp	0.825	0.4125	0.3209	1.29	0.268
Force	3.325	1.6625	0.3209	5.18	0.007
Bonding Time	-0.075	-0.0375	0.3209	-0.12	0.913
R-Sq =		87.70%			

The electromechanical performance of the electrostatic actuator array was also evaluated for each sample bonded in the DOE. After TWV and interposer assembly, the chip stack was packaged using the PGA carrier shown in Figure 10. This package is compatible with BMC MultiDM driver technology, which was used to supply high voltage to the actuators on the TWV die one at a time. Actuator failures are caused by failed flip-chip connections, damaged wires on the surface of the interposer die, or manufacturing problems with the fabrication of the actuator array. From these tests it was determined that actuator yield was highly correlated with bonds that experienced a small changing in die curvature. Samples with more than 5 meters radius of curvature change yielded poorly (sample # 3, 4, 6, and 8 – all less than 50% yield – some with noticeable actuator damage) and another sample (# 2) with a slightly higher yield (82%) also experienced significant curvature change (3.5m). Sample #5 had the highest actuator yield (92%) and experienced the least amount of curvature change (2m). This sample was bonded using the low force, low temperature, high time split of the DOE.

The deflection behavior of several actuators from each of the bonded and packaged DOE devices was also evaluated in this work. The applied voltage and deflection behavior of an actuator from sample #5 can be seen in Figure 11. The inset of Figure 11 shows an interferometric image of an actuator deflected by 1.2um at 250V.

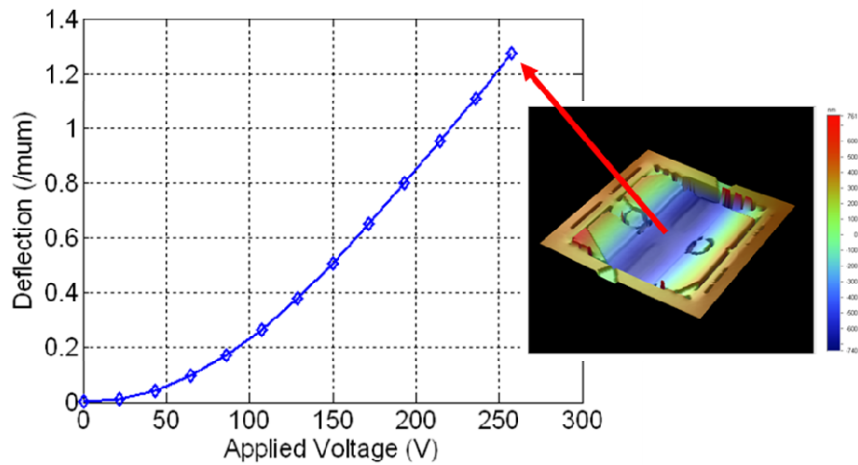


**Figure 11:** Voltage vs. deflection of a central actuator from sample # 5.

In addition to measuring the change in die curvature as a result of the bonding process, a change in unpowered actuator position after bonding also provides a means of inferring stress in the device. The displacement of the actuator center relative to its anchors (sides) is called the actuator sag and it was recorded for all of the devices bonded in the DOE above. A summary of the results are listed in Table 4. Unlike actuator yield, we do not see a large correlation of sag change with actuator yield or die curvature. For this reason, it was not selected as the response factor for the DOE.

**Table 4:** Post bonding actuators sag at center and corner. Values for curvatures shown for comparison.

Sample #	Radius of curvature change (m)	Sag (nm)	
		Center	Corner
Before bonding		-300	-312
1	3.5	NA	NA
2	3.5	-182	-325
3	7	-296	-328
4	6.8	-245	-320
5	2	-175	-398
6	5	-230	-290
7	6.5	-310	-390
8	7	-279	-330

## 5. Conclusions

A successful thermo-compression flip-chip assembly and packaging process for bonding DM electrostatic actuator arrays with TWV interconnects to interposer die has been developed. The methodology of using an interposer board for reducing connection density was also demonstrated to be useful. A flip-chip process capable of producing low stress bonded die was developed and is expected to be successful for fully functional DMs with greater actuator counts. Lastly, the initial process development of an adhesive flip-chip bonding approach has also been completed and also appears to have promise for full scale flip-chip packaging of high actuator count DMs.

## References

- [1] Cornelissen, S.,A., et. al., "4096-element face-sheet MEMS deformable mirror for high-contrast imaging," *Journal Micro Nanolith. MEMS MOEMS* 8 , (2009)
- [2] Rimskog, M., "Through wafer via technology for MEMS 3D integration," *Electronic Manufacturing Technology Symposium*, (2007)
- [3] Rimskog, M., Bauer, M., "High density through wafer via technology," *DTIP of MEMS & MOEMS*, (2008)
- [4] Frederick, S., McCormick, F.,B., "Integrated optical MEMS using through-wafer vias and bump-bonding," *Sandia National Laboratories Report*, (2008)
- [5] Tsau, C.,H., Spearing, S.,M., Schmidt, M.,A., "Characterization of wafer-level thermocompression bonds," *Journal of Microelectromechanical Systems* 13 (6), 963-971 (2004)
- [6] Lau, J.,H., [Flip Chip Technologies], McGraw-Hill, New York (1995)